Crystallographic Studies of the Catalytic Mechanism of the Neutral Form of Fructose-1,6-bisphosphatase†

Yiping Zhang, Jiin-Yun Liang, Shenghua Huang, Hengming Ke,‡ and William N. Lipscomb*

Gibbs Chemical Laboratory, Harvard University, 12 Oxford Street, Cambridge, Massachusetts 02138

Received September 15, 1992; Revised Manuscript Received November 19, 1992

ABSTRACT: The crystal structures of fructose-1,6-bisphosphatase (EC 3.1.3.11) complexed with substrate alone or with substrate analogues in the presence of divalent metal ions have been determined. The substrate analogues, 2,5-anhydro-D-glucitol-1,6-bisphosphate (AhG-1,6-P_2) and 2,5-anhydro-D-mannitol-1,6-bisphosphate (AhM-1,6-P_2), differ from the α and β anomers of fructose-1,6-bisphosphate (Fru-1,6-P_2), respectively, in that the OH on C2 is replaced by a hydrogen atom. Structures have been refined at resolutions of 2.5 to 3.0 Å to *R* factors of 0.172 to 0.195 with root-mean-square deviations of 0.012–0.018 Å and 2.7–3.8° from the ideal geometries of bond lengths and bond angles, respectively. In addition, the complex of substrate with the enzyme has been determined in the absence of metal. The electron density at 2.5-Å resolution does not distinguish between α and β anomers, which differ for the most part only in the position of the 1-phosphate group and the orientation of the C2-hydroxyl group. The positions of the 6-phosphate and the sugar ring of the substrate analogues are almost identical to those of the respective anomer of the substrate. In the presence of metal ions the positions of the 1-phosphate groups of both α and β analogues differ significantly (0.8–1.0 Å) from those of anomers of the substrate in the metal-free complex. Two metal ions (Mn^{2+} or Zn^{2+}) are located at the enzyme active site of complexes of the α analogue AhG-1,6-P_2. Metal site 1 is coordinated by the carboxylate groups of Glu-97, Asp-118, and Glu-280 and the 1-phosphate group of substrate analogue, while the metal site 2 is coordinated by the carboxylate groups of Glu-97, Asp-118, the 1-phosphate group of substrate analogue, and the carbonyl oxygen of Leu-120. Both metal sites have a distorted tetrahedral geometry. However, only one metal ion (Mg^{2+} or Mn^{2+}) is found very near the metal site 1 in the enzyme's active site in complexes of the β analogue AhM-1,6-P_2 or for Mg^{2+} in the complex of the α analogue AhG-1,6-P_2. This single metal ion is coordinated by the carboxylate groups of Glu-97, Asp-118, Asp-121, and Glu-280 and the 1-phosphate group of substrate analogue in a distorted square pyramidal geometry. A possible mechanism is favored in which a metal-activated water molecule attacks the 1-phosphate of the α anomer of the substrate, while a proton is transferred from the unionized side chain carboxyl group of Asp-121 to the substrate ester oxygen O1 directly or through the help of the C2-hydroxyl group of the substrate, thus weakening the P–O bond. This mechanism is consistent with experimental results of others: only the α anomer of substrate is hydrolyzed by the enzyme, the enzyme can bind two Mn^{2+} or Zn^{2+} ions at the active site in the presence of substrate or its analogue, the phosphate group is transferred to water directly with inversion at the phosphorus center, and the C2-hydroxyl group of substrate is absolutely required for activity. However, questions remain about the catalytic mechanism which is implied by the single-site Mg^{2+} complex with enzyme and substrate analogue. Amino acid candidates for site-directed mutagenesis are proposed.

Fructose-1,6-bisphosphatase (Fru-1,6-Pase, E.C. 3.1.3.11)[1] is a key regulatory enzyme in the gluconeogenesis pathway. It catalyzes the hydrolysis of D-fructose-1,6-bisphosphate (Fru-1,6-P_2) to D-fructose-6-phosphate (Fru-6-P) and inorganic phosphate in the presence of a divalent metal ion, such as magnesium, manganese, or zinc. The activity of the enzyme is regulated by two inhibitors: AMP and fructose-2,6-bisphosphate (Fru-2,6-P_2). The enzyme is activated by divalent metal ions, such as Mg^{2+}, Mn^{2+}, Co^{2+}, or Zn^{2+}, at low concentrations (Benkovic & deMaine, 1982; Tejwani, 1983; Kirley & Dix, 1971) but inhibited by higher concentrations of Mg^{2+}, Mn^{2+}, and Zn^{2+} (Rack & Shroeder, 1958; Underwood & Newsholme, 1965; Van Tol et al., 1972; Marcus et al., 1973; Han et al., 1975; Benkovic et al., 1978a).

Fru-1,6-Pase is a tetramer having D_2 symmetry. The crystal structures of product Fru-6-P complex (R form), active site inhibitor Fru-2,6-P_2 complex (R form), and allosteric inhibitor AMP complex (T form) have been solved previously in this laboratory (Ke et al., 1990a,b, 1991a,b; Liang et al., 1992). The substrate, product, competitive inhibitor Fru-2,6-P_2, and the metal ions all bind at or very near the active site. AMP binds at an allosteric site about 28 Å from the nearest active site, and this binding causes the R to T transition: a 17° rotation of the lower dimer relative to the upper dimer in the quaternary structure. Significant changes occur at the AMP and the metal binding sites as AMP binds (Ke et al., 1990b, 1991a; Lipscomb, 1991).

The substrate Fru-1,6-P_2 exists mainly in two slowly equilibrating anomeric forms in solution, consisting of about 15% α anomer and 79% β anomer (Midelfort et al., 1976).

Rapid quench kinetic studies using Mn^{2+} as the activating cation showed that the catalytic reaction proceeds in two phases: first a rapid formation of the product, corresponding

† This work is supported by NIH Grant GM 06920.

* To whom correspondence should be addressed.

‡ Present address: Department of Biochemistry and Biophysics, School of Medicine, The University of North Carolina, Chapel Hill, NC 27599.

[1] Abbreviations: Fru-1,6-Pase, fructose-1,6-bisphosphatase; Fru-1,6-P_2, fructose-1,6-bisphosphate; Fru-2,6-P_2, fructose-2,6-bisphosphate; Fru-6-P, fructose-6-phosphate; AhG-1,6-P_2, 2,5-anhydro-D-glucitol-1,6-bisphosphate; AhM-1,6-P_2, 2,5-anhydro-D-mannitol-1,6-bisphosphate; 5-d-Fru-1,6-P_2, 5-deoxyfructose-1,6-bisphosphate; Xylu-1,5-P_2, xylulose-1,5-bisphosphate.

0006-2960/93/0432-1844$04.00/0

Table I: Summary of Crystallographic Parameters for Data Collection, Reduction, and Refinements[a]

	AMMG	AMMN	AGMG	AGMN	AGZN	F16P
a, b (Å)	131.4	132.0	131.4	131.6	132.0	131.2
c (Å)	69.2	67.4	68.9	68.3	67.4	69.3
total refl. no.	57091	76629	60251	59064	54498	94675
uniq. refl. no.	17456	13551	17881	11800	13324	24277
R_{merge}	5.7%	6.6%	6.7%	7.1%	6.3%	7.7%
resolution (Å)	2.7	3.0	2.6	2.9	3.0	2.5
completeness	87.5%	91.5%	82.4%	75.8%	90.4%	91.2%
rms of bond (Å)	0.014	0.015	0.016	0.015	0.018	0.012
rms of angle (deg)	3.14	3.62	3.35	3.53	3.82	2.70
R factor	0.189	0.190	0.185	0.172	0.195	0.193

[a] $R_{merge} = \sum_{hkl}\sum_i|I_i - \langle I\rangle|/\sum_{hkl}\langle I\rangle$. Abbreviations used in this and the following tables: AGMG, AhG-1,6-P_2–Mg–Fru-1,6-Pase; AGMN, AhG-1,6-P_2–Mn–Fru-1,6-Pase; AGZN, AhG-1,6-P_2–Zn–Fru-1,6-Pase; AMMG, AhM-1,6-P_2–Mg–Fru-1,6-Pase; AMMN, AhM-1,6-P_2–Mn–Fru-1,6-Pase; F16P, Fru-1,6-P_2–Fru-1,6-Pase.

to about 18% of available substrate, followed by a slow reaction which has an apparent rate independent of the enzyme concentration and close to that of the nonenzymatic conversion between α and β anomers in solution (Benkovic et al., 1974; Frey et al., 1977). These authors therefore suggested that the α anomer is the true substrate and that the β anomer is probably converted nonenzymatically to the α anomer before it can be hydrolyzed. On the other hand, results from kinetic studies of bovine hepatic Fru-1,6-Pase using substrate analogues 2,5-anhydro-D-glucitol-1,6-bisphosphate (AhG-1,6-P_2, analogue of α anomer) and 2,5-anhydro-D-mannitol-1,6-bisphosphate (AhM-1,6-P_2, analogue of β anomer) (Figure 1) showed that the K_i for the β analogue is 20 times lower than the K_i for the α analogue, suggesting that the β anomer may be the major substrate (Marcus, 1976). Also, the mechanisms of inhibition by metal ions at high concentrations are not well understood. Nor is it clear how Zn^{2+} ion at a low micromolar concentration range inhibits the enzyme when the activating metal ion is Mg^{2+} or Mn^{2+}, while this same inhibition could be reversed by Zn^{2+} at above 10 μM concentration, although the final enzyme activity is still lower than that of the Mg^{2+}- or Mn^{2+}-activated enzyme.

The present study was carried out in order to address these questions and to provide structural information about the catalytic mechanism. We report here refined structures of Fru-1,6-Pase complexed with substrate Fru-1,6-P_2 and of various ternary complexes of Fru-1,6-Pase with divalent metal ions and substrate analogues. On the basis of these results, a possible catalytic mechanism is proposed.

MATERIALS AND METHODS

AhG-1,6-P_2 was synthesized according to Hartman and Barker (1965) and was at least 98% pure as shown by ^{31}P NMR spectroscopy. AhM-1,6-P_2 was kindly provided by Dr. Thomas Claus. Fru-1,6-P_2 was purchased from Sigma Chemical Co. and used without further purification. Ultrapure $MgCl_2$ (99.999%), $MnCl_2$ (99.99%), and $ZnCl_2$ (99.999%) were purchased from Aldrich Chemical Co. Pig kidney Fru-1,6-Pase was purified as described previously (Ke et al., 1990a,b). In order to prepare various complexes, crystals of the Fru-6-P complex, grown as previously described (Ke et al., 1991b), were soaked for 3–5 days at pH 7.4 in a buffer containing 20.0 mM Tris, 20% PEG (mean molecular mass 3350 Da), 5.0 mM NaN_3, 1.0 mM 2-mercaptoethanol, 0.5 mM substrate analogue (AhG-1,6-P_2 or AhM-1,6-P_2), and one choice of the divalent metal ions ($MgSO_4$, 5.0 or 20.0 mM; $MnCl_2$, 0.5 mM; $ZnCl_2$, 5.0 μM). All of the complexes were isomorphous with the Fru-6-P complex in the space group $P3_221$ which has two subunits, designated C1 and C2, in the crystallographic asymmetric unit (Table I).

The diffraction data (Table I) of AhG-1,6-P_2 and AhM-1,6-P_2 complexes were collected on the Siemens multiwire area detector at the Gibbs Laboratory of Harvard University with use of the Harvard data collection software (Blum et al., 1987). Data scaling and reduction to structure factors were performed using the algorithm of Fox and Holmes (1966) as implemented in programs ROTAVATA and AGROVATA of the CCP4 program package (CCP4, 1979). The diffraction data for the Fru-1,6-P_2 complex were collected on the multiwire X-ray area detector at the Biotechnology Resource, University of Virginia (Sobottka et al., 1984).

The coordinates of the Fru-6-P complex at 2.1-Å resolution (Ke et al., 1991b) were used as the initial model for all the complexes, and the structures were rebuilt as necessary using the program FRODO (Jones et al., 1982) on a PS390 Graphics workstation connected to a VAX computer. Bond lengths and bond angles for Fru-1,6-P_2, taken from the literature (Narendra et al., 1985; Cerrini et al., 1986), were held fixed during the refinements. The furanose ring of β Fru-1,6-P_2 was fixed at the C2-exo conformation as observed in its crystal structure. For the α Fru-1,6-P_2, the furanose ring was assigned a conformation of C3-endo, the preferred conformation for furanose rings in nucleotides. Coordinates for the analogues AhG-1,6-P_2 and AhM-1,6-P_2 are derived from the coordinates of the corresponding anomer of Fru-1,6-P_2 by eliminating the O2 oxygen atom.

The initial metal ion positions were located from $(F_o - F_c)$ difference Fourier maps, where F_c was calculated using the coordinates of the Fru-6-P complex. Positional and temperature factors were then refined using program X-PLOR (Brünger et al., 1987). In Table I, we give the bond length and bond angle deviations from their ideal values and also include the refined crystallographic residue R factors.

RESULTS

From the $(F_o - F_c)$ difference maps, the electron density for the substrate or its analogues in the active site are well-defined and are at least five times the average background density. The electron densities for metal ions are also well-defined and are over 8 times the background density for zinc and manganese complexes and about 5 times the background density for magnesium complexes. The structures of both substrate anomers and their respective analogues are given in Figure 1. The active site residues that interact with substrate or its analogues are summarized in Table II.

The active site can be divided into three parts, the 6-phosphate binding region, sugar ring binding region, and 1-phosphate and metal binding region (Figure 2). Superposition of the active site residues gives almost identical positions and binding for side chains that interact with the

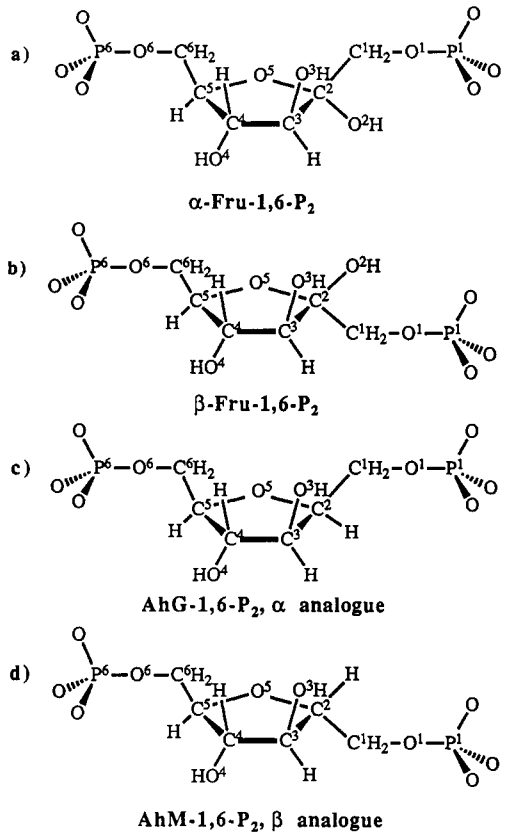

FIGURE 1: Schematic drawings of substrate Fru-1,6-P_2, (a) α anomer and (b) β anomer, and the substrate analogues (c) α analogue AhG-1,6-P_2 and (d) β analogue AhM-1,6-P_2.

6-phosphate and sugar ring groups in substrate and analogue complexes. For metal binding residues, rms shifts of Cα atoms of 0.5–0.8 Å are observed when metal ions bind. Substantial differences are observed for the 1-phosphate groups mostly due to anomeric differences. Moreover, the positions for the 1-phosphate shown in Figure 2 are further changed upon metal binding. Detailed interactions of substrate, substrate analogues, and metal ions in the active site are given below.

(*a*) *Structure of Fru-1,6-P_2 Complex.* The ($F_o - F_c$) density for the substrate in its metal-free complex with Fru-1,6-Pase can be fitted equally well with either the α or β anomer of Fru-1,6-P_2 (Figure 3). From the shape of this density at 2.5-Å resolution, it is impossible to distinguish which anomer is bound at the active site or, if both anomers are present, what the proportion is for each anomer.

For the purpose of refinement and in order to compare the density with both anomers, we modeled α and β anomers of substrate at the active site with assumed occupancies of 0.20 and 0.80, respectively. The positions of the 6-phosphate are almost identical in the two anomers, and so are the positions of the furanose ring. Also, the same polar interactions with the active site residues in both anomers are observed for the 6-phosphate and the sugar ring. For example, the 6-phosphate group forms hydrogen bonds with the side chain OH groups of Tyr-215, Tyr-244, and Tyr-264 and with the NH_2 of Asn-212. Also, a side chain NH_2^+ of Arg-243 from the neighboring C2 chain forms a salt bridge with the 6-phosphate oxygen O21 (Figure 2).

The binding domain of the sugar ring consists of Asp-121, Met-248, and Lys-274. The sugar ring is apparently less tightly bound than is the 6-phosphate and may have relatively more freedom of movement (see Discussion). The hydroxyl group on C3 forms two hydrogen bonds, one to the main chain NH of Met-248 and the other to the carboxylate oxygen Od2 of Asp-121 (Figure 2). The NH_3^+ of Lys-274 plays a critical role in binding of the substrate, and is even more important in binding of the competitive inhibitor Fru-2,6-P_2 (Liang et al., 1992; Raafat et al., 1992). This group donates two hydrogen bonds to bridging oxygen atoms O5 and O6 of the substrate and it also interacts with the 2-phosphate group of Fru-2,6-P_2, forming a salt bridge (Liang et al., 1992).

The positions of the 1-phosphate group are different in the two anomers. The distance from the 1-phosphorus atom to the sugar ring in the β anomer is about 0.7 Å longer than that in the α anomer. In both anomers the 1-phosphate forms hydrogen bonds with the carboxylate group of Asp-121 and with the main chain NH of Gly-122. Also, in the α anomer of the substrate there is a salt bridge between the 1-phosphate oxygen O11 and a side chain $NH_2^{\delta+}$ of Arg-276 in the C1 chain but not in the C2 chain.

(*b*) *Structure of AhG-1,6-P_2 Complexes.* In the AhG-1,6-P_2–M–Fru-1,6-Pase complexes (M = Mg^{2+}, Mn^{2+}, or Zn^{2+}), the 6-phosphate groups are located at the same positions as in the α Fru-1,6-P_2 complex and have identical interactions with its surrounding residues regardless of which metal is present at the metal binding sites. However, in the presence of metal ions the position of the 1-phosphate groups is different from that of the 1-phosphate group in the α Fru-1,6-P_2 complex (Figure 4). In the three complexes with metal ions, the 1-phosphate groups are bound to one (Mg^{2+}) or to two metal ions in either the Mn^{2+} or Zn^{2+} complexes. The average distance between phosphorus atoms of the 1-phosphate and 6-phosphate groups in α Fru-1,6-P_2, AhG-1,6-P_2 with Mg^{2+}, and AhG-1,6-P_2 with Mn^{2+} or Zn^{2+} are 7.9, 8.6, and 9.1 Å, respectively. To accommodate these differences, dihedral angle changes about several bonds (such as C5–C6, C6–O6, O1–C1, and C1–C2) of AhG-1,6-P_2 are necessary, resulting in slight changes of orientation and position of the sugar ring. The hydroxyl group on C3 still has similar hydrogen bond interactions with residues Asp-121 and Met-248 in these complexes. The side chain $NH_2^{\delta+}$ of Arg-276 no longer interacts with the 1-phosphate oxygen atoms because the phosphate group has moved toward metal binding sites. Finally, the main chain NH of Gly-122 forms a bifurcated hydrogen bond to the ester oxygen O1 and a 1-phosphate oxygen O12 (2.6 Å to O1 and 2.5 Å to O12).

(*c*) *Structure of AhM-1,6-P_2 Complexes.* In the AhM-1,6-P_2–M–Fru-1,6-Pase (M = Mg^{2+} or Mn^{2+}) complexes, the 6-phosphate and the sugar ring of AhM-1,6-P_2 are bound as in the substrate and the α analogue AhG-1,6-P_2 complexes. The average distance between phosphorus atoms of the 1-phosphate and the 6-phosphate groups are 8.0, 8.3, and 8.8 Å, respectively, in complexes of β Fru-1,6-P_2, AhM-1,6-P_2 with Mg^{2+}, and AhM-1,6-P_2 with Mn^{2+}. The phosphate oxygen O12 is about 3.0 Å from the main chain NH of Gly-122, 0.5 Å longer than the distance between these two atoms in AhG-1,6-P_2 complexes but still within hydrogen bonding distance, and oxygen O11 is coordinated to the metal ions (Figure 5). There is no interaction between the ester oxygen O1 and the main chain NH group of Gly-122.

(*d*) *Metal Binding Sites.* Two metal binding sites were located by the difference Fourier synthesis method at the active site in the ternary complexes of AhG-1,6-P_2–M–Fru-1,6-Pase with M = Mn^{2+} or Zn^{2+}. The two metal ions are bonded by the carboxylate groups of Glu-97 and Asp-118 and the 1-phosphate group of AhG-1,6-P_2. All three of these groups act as bridging bidentate ligands (Table II, part c, and Figures 4 and 6a). The fourth ligands of metals 1 and 2 are the

Table II

a. Interactions between α-Fru-1,6-P_2 or AhG-1,6,-P_2 and the Active Site Residues

	AGMG		AGMN		AGZN		α-F16P	
atoms	C1[a]	C2[a]	C1[a]	C2[a]	C1[a]	C2[a]	C1[a]	C2[a]
Asp-121 OD1	O1		O1	O1		O1		
Asp-121 OD1							O2	O2
Asp-121 OD1	O11[c]	O11						
Asp-121 OD2	O3	O3	O3	O3	O3	O3	O3	
Gly-122 N	O12	O12	O12	O12	O12	O12		
Gly-122 N			O1	O1	O1	O1		
Asn-212 ND2				O21			O21	O21
Asn-212 ND2	O22	O22	O22	O22	O22	O22	O22	O22
Tyr-215 OH	O23	O23	O23	O23	O23	O23	O23	O23
Arg-243 NH1[b]	O21	O21	O21	O21	O21	O21	O21	O21
Arg-243 NH2[b]		O21	O21	O21		O21	O21	O21
Arg-243 NH2[b]								O22
Tyr-244 OH	O22	O22	O22	O22	O22	O22	O22	O22
Met-248 N	O3		O3	O3	O3	O3	O3	O3
Tyr-264 OH	O23	O23	O23		O23	O23	O23	O23
Lys-274 NZ	O5	O5	O5	O5	O5	O5	O5	O5
Lys-274 NZ	O6	O6	O6	O6	O6	O6		
Arg-276 NH1							O2	

b. Interactions between β-Fru-1,6-P_2 or AhM-1,6,-P_2 and the Active Site Residues

	AMMG		AMMN		β-F16P	
atoms	C1	C2	C1	C2	C1	C2
Asp-121 OD1			O3	O3		O3
Asp-121 OD1	O11	O11				
Asp-121 OD1			O12	O12	O12	
Asp-121 OD2		O3	O3	O3	O3	O3
Gly-122 N	O12	O12	O12	O12	O12	O12
Asn-212 ND2		O22		O22	O22	O22
Tyr-215 OH		O22	O22			
Tyr-215 OH	O23	O23		O23	O23	O23
Arg-243 NH1	O21	O21			O21	O21
Arg-243 NH2	O21				O21	O21
Tyr-244 OH	O22	O22		O22	O22	O22
Met-248 N	O3	O3	O3	O3	O3	O3
Tyr-264 OH	O23	O23			O23	O23
Lys-274 NZ	O6			O6	O6	

c. Interactions between Metal Ions and Active Site Residues

	AGMG		AGMN		AGZN		AMMG		AMMN	
atoms	C1	C2	C1	C2	C1	C2	C1	C2	C1	C2
Glu-97 OE2	MG	MG					MG	MG		
Asp-118 OD2	MG	MG					MG	MG		
Asp-121 OD1	MG	MG					MG	MG		
Glu-280 OE1	MG	MG					MG	MG		
AhG-336 O11	MG									
AhG-337 O11		MG								
AhM-336 O11							MG			
AhM-337 O11								MG		
Glu-97 OE2			MN1	MN1					MN	MN
Asp-118 OD2			MN1	MN1					MN	MN
Glu-280 OE1			MN1	MN1					MN	MN
AhG-336 O11			MN1							
AhG-337 O11				MN1						
AhM-336 O11									MN	
AhM-337 O11										MN
Asp-121 OD1									MN	MN
Glu-97 OE1			MN2	MN2						
Asp-118 OD1			MN2	MN2						
Leu-120 O			MN2	MN2						
AhG-336 O12			MN2							
AhG-337 O12				MN2						
Glu-97 OE2					ZN1	ZN1				
Asp-118 OD2					ZN1	ZN1				
Glu-280 OE1					ZN1	ZN1				
AhG-336 O11					ZN1					
AhG-337 O11						ZN1				
Glu-97 OE1					ZN2	ZN2				
Asp-118 OD1					ZN2	ZN2				
Leu-120 O					ZN2	ZN2				
AhG-336 O12					ZN2					
AhG-337 O12						ZN2				

[a] In this and following tables, C1 and C2 refer to the two monomers in the crystallographic asymmetric unit. [b] Arg-243 is from the neighboring chain. [c] O11, O12, and O13 are 1-phosphate oxygens; O21, O22, and O23 are 6-phosphate oxygens.

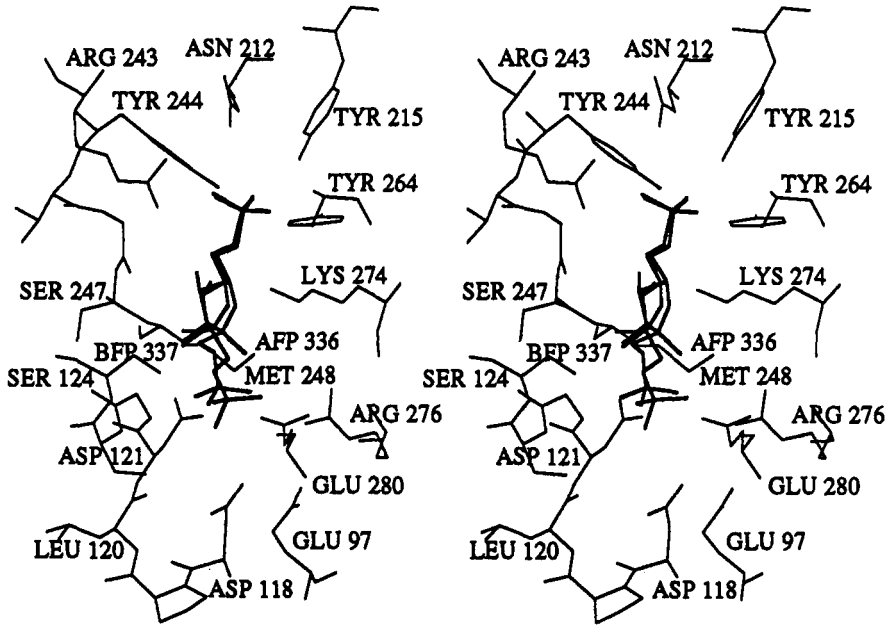

FIGURE 2: Stereo plot of the active site with both α and β Fru-1,6-P_2 in the metal-free complex. AFP-336 denotes the α anomer and BFP-337 denotes the β anomer. The β anomer is the more extended structure.

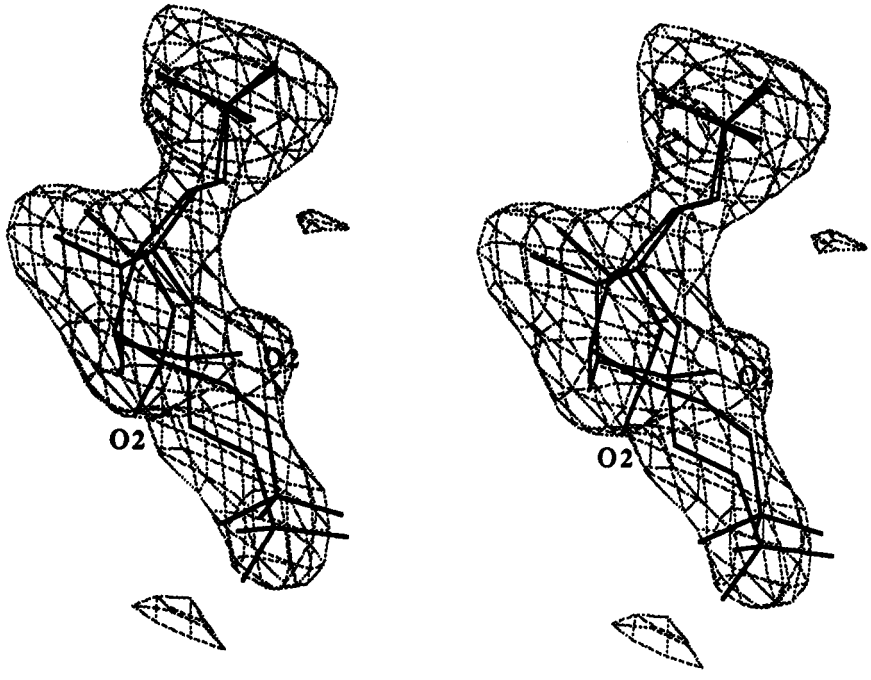

FIGURE 3: Model of both α and β Fru-1,6-P_2 built into the electron density in the ($F_o - F_c$) map calculated by omitting both anomers. The map is contoured at the 3σ level. Atom O2 on the right belongs to the β anomer, and atom O2 on the left belongs to the α anomer. In this and all the subsequent figures, the 6-phosphate group is at the top and the 1-phosphate group is at the bottom of the picture.

carboxylate oxygen Od2 of Glu-280 and the carbonyl oxygen of Leu-120, respectively. The carboxylate group of Asp-121 is nearby at about 2.8 Å from the metal site 1. In the various structures, the distances between the two metal ions are in the range 3.6–3.8 Å. Both metal ions have a distorted tetrahedral geometry, where the most open face which is not in the direction of the other metal is opposite to atoms Oe2 of Glu-97 and Od1 of Asp-118 for metal sites 1 and 2, respectively.

In the ternary complexes of AhG-1,6-P_2–Mg^{2+}–Fru-1,6-Pase and AhM-1,6-P_2–M^{2+}–Fru-1,6-Pase (M = Mg^{2+} or Mn^{2+}), only one metal binding site was found. This site is very near the metal site 1 in the AhG-1,6-P_2–M–Fru-1,6-Pase complexes (M = Zn^{2+} or Mn^{2+}). This single metal ion is coordinated by carboxylate oxygen atoms of Glu-97, Asp-118, Asp-121, and Glu-280 and the 1-phosphate oxygen O11 of AhG-1,6-P_2 or AhM-1,6-P_2 in a distorted square pyramidal geometry. The same result was obtained for the complex AhG-1,6-P_2–Mg^{2+}–Fru-1,6-Pase when the $MgSO_4$ concentration in the buffer solution used for preparing the crystals was increased from 5.0 mM to 20.0 mM.

For all of the complexes there is electron density in the ($F_o - F_c$) difference maps at one of the two AMP binding sites in the crystallographic asymmetric unit, in C1 but not in C2. These densities arise from low-occupancy binding of the substrate or substrate analogues at the AMP site. Because of the relatively low resolution of the diffraction data and low occupancy of the site, we did not include them for the refinements. However, no metal ions were visible in our maps at these AMP sites.

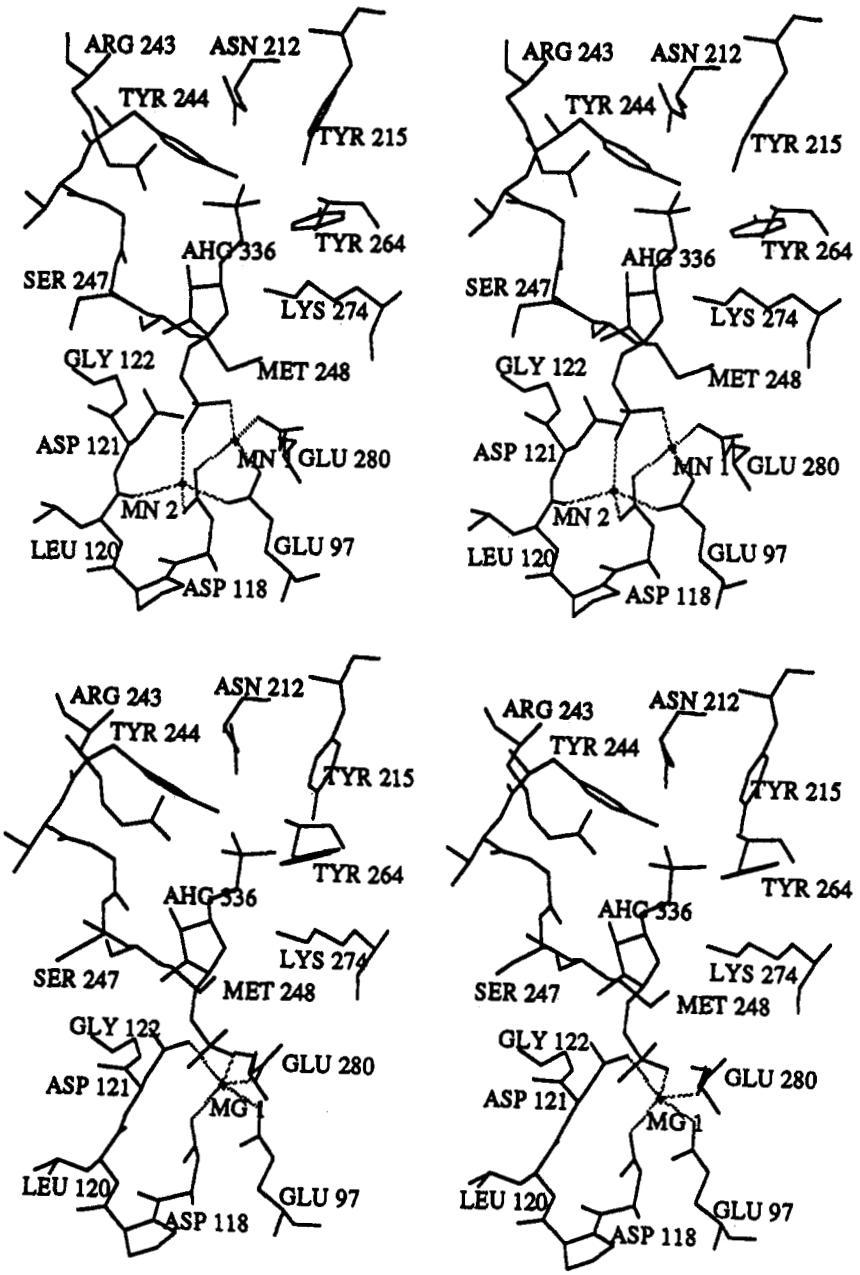

FIGURE 4: Stereo plot of the active site with the α analogue AhG-1,6-P_2 in the presence of (a, top) 0.5 mM Mn^{2+} showing 2 Mn^{2+} ions (very near the same position as those for 5.0 μM Zn^{2+}) and (b, bottom) 5.0 mM or 20.0 mM Mg^{2+} showing one Mg^{2+}. Bonds between the metal ions and the ligands are represented by dotted lines.

DISCUSSION

(*a*) *Binding of Substrate and Its Analogues.* The polar interactions between the active site residues and the substrate or its analogues are represented schematically in Figure 7.

In solution, Fru-1,6-P_2 exists in an equilibrium between α anomer (15%), β anomer (81%), acyclic keto (2%), and gem diol (1.3%) forms (Midelfort et al., 1976). Initially, only the β anomer was modeled in the refinements of the data obtained in the absence of metal ions. Upon examining the model, we observed that the 1-phosphate group is not strongly bound to the active site residues and that it has considerable flexibility as indicated by the average *B* factors[2] for 6-phosphate, sugar ring, and 1-phosphate groups of 22, 30, and 75 Å^2, respectively. For comparison, average *B* factors for the side chains of active site residues are in the range of 15–45 Å^2. So in later stages of refinement of this complex, we modeled both the α and β anomers, with occupancies of 0.2 and 0.8, respectively. The 6-phosphate groups and sugar rings were located at their respective sites in both anomers. Of course, the hydroxyl groups on carbon atom C2 are on the opposite sides of the sugar ring so that the 1-phosphate group is 0.7 Å further away from the sugar-6-phosphate portion in the β anomer, as compared to the location in the α anomer. Moreover, the presence of metal ions causes a further shift of the position of the 1-phosphate group in the same direction toward the metal ions (Figure 8). The orientations of the 1-phosphate groups, of course, are different in the two anomers. In the AhG-1,6-P_2 complexes with Zn^{2+} or Mn^{2+}, the 1-phosphate group is oriented so that it can act as a bridging ligand with O11 and O12 coordinated to metal 1 and metal 2, respectively. On the other hand, in the AhM-1,6-P_2 complexes, the orientation of the 1-phosphate is such that only one oxygen

[2] The temperature disorder factor *B* is $8\pi^2\mu^2$, where $\sqrt{\mu^2}$ is the root mean square of apparent amplitude of motion or disorder.

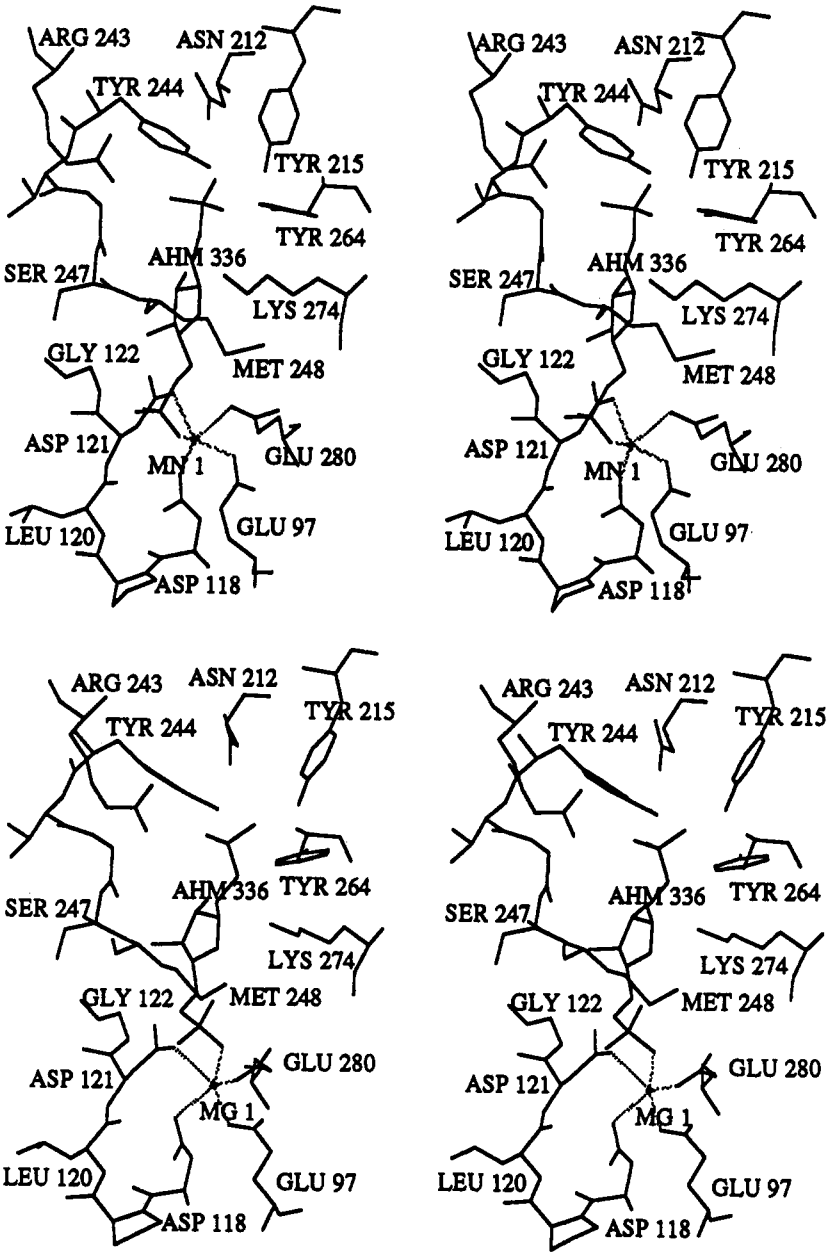

FIGURE 5: Stereo plot of the active site with the β analogue AhM-1,6-P_2 in the presence of (a, top) 0.5 mM Mn^{2+} showing one Mn^{2+} and (b, bottom) 5.0 mM Mg^{2+} showing one Mg^{2+}. Bonds between metal ion and ligands are represented by dotted lines.

atom is suitable for coordination to the metal: O11 binds to the metal at site 1. This difference in orientation of the 1-phosphate group is at least partly responsible for the occurrence of only one metal binding site at the active site of AhM-1,6-P_2 complexes. In addition, there is a bifurcated hydrogen bond interaction with the main chain NH group of Gly-122 as the donor and both the ester oxygen O1 and a phosphate oxygen O12 as acceptors in the AhG-1,6-P_2 complexes with Zn^{2+} or Mn^{2+}. This hydrogen bond may help to anchor the 1-phosphate group at the required position for metal binding and catalysis. The NH group of Gly-122 is hydrogen bonded only to the oxygen O12 of the 1-phosphate in either of the two AhM-1,6-P_2 complexes or in the AhG-1,6-P_2 complex with Mg^{2+} or in the metal-free substrate complex.

These results suggest that the binding step at the active site does not have a strong anomeric specificity. The enzyme appears to bind both anomers in the presence or absence of metal ions, although we cannot be sure of the ratio. The mutual enhancement between metal binding and substrate binding observed in kinetic studies is a direct consequence of the interactions between the 1-phosphate group and metal ions at the active site. The findings that two Zn^{2+} or Mn^{2+} ions (but only one Mg^{2+}) are bound in the presence of the α analogue AhG-1,6-P_2 and that only one Mg^{2+} or Mn^{2+} is bound in the presence of the β analogue AhM-1,6-P_2 lend support to the conclusions that the enzyme binds the α anomer more strongly than the β anomer in rapid quench experiments in which Mn^{2+} is the activator (Caperelli et al., 1978).

(*b*) *Binding of Divalent Metals.* Various kinetic studies of the binding of divalent metal ions to Fru-1,6-Pase have been reported. In summary, one to three Zn^{2+} ions were found to bind to each monomer of the enzyme from various sources in the presence or absence of substrate, product, or their analogues (Tejwani et al., 1976; Benkovic et al., 1978a; Pontremoli et al., 1978, 1979; Ikeda et al., 1980). For manganese binding, one metal was bound per monomer in the absence of substrate, or two metal ions were bound to each monomer in the presence of substrate or its analogues (Pontremoli et al., 1969; Grazi et al., 1971; Libby et al., 1975; Benkovic et al., 1978b). The

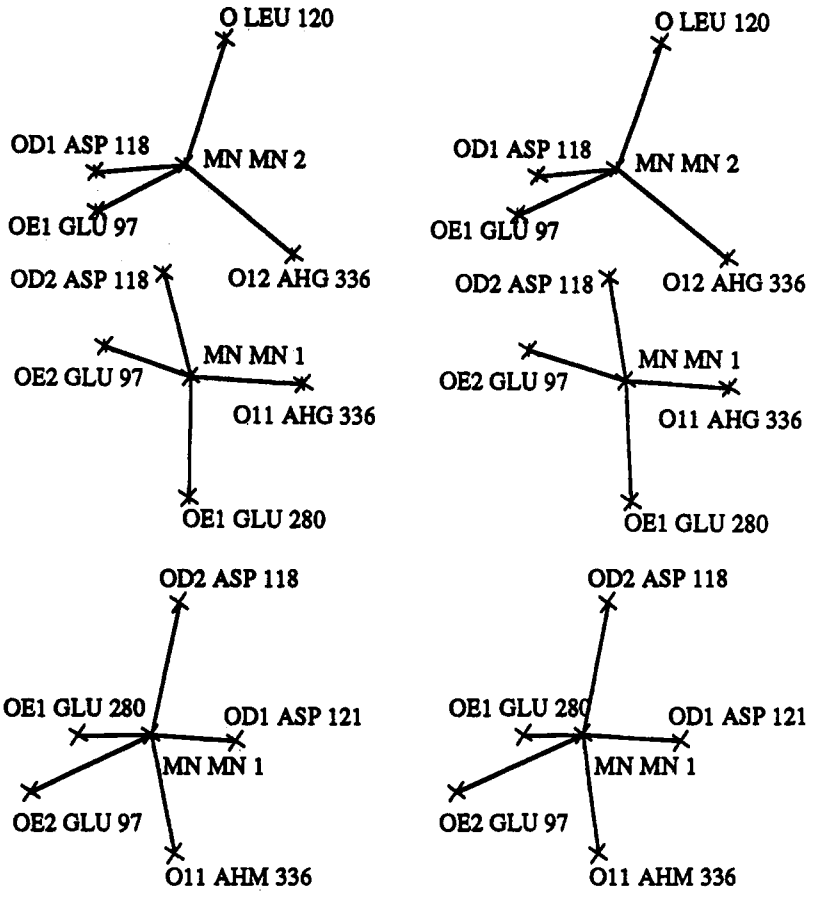

FIGURE 6: Metal binding sites in stereo view: (a, top) in AhG-1,6-P_2-Mn-Fru-1,6-Pase and (b, bottom) in AhM-1,6-P_2-Mg-Fru-1,6-Pase.

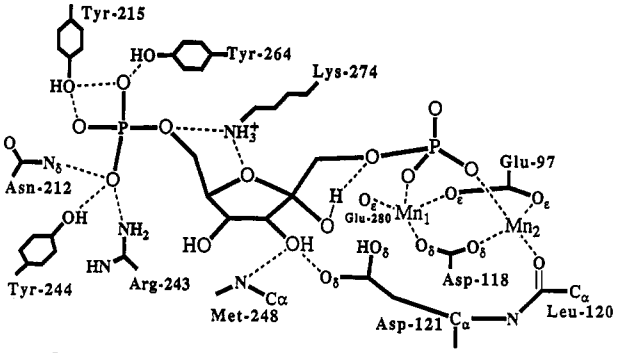

FIGURE 7: Schematic representation of the substrate binding site in the presence of divalent metal ions. Dotted lines denote hydrogen bond interactions.

enzyme became fully active only after the second metal ion was bound. On the basis of the kinetic and binding experiments, the first set of four strongly bound metal ions per tetramer molecule are designated as "structural" metal and the second set of four less strongly bound metal ions as "catalytic" metal (Grazi et al., 1971; Libby et al., 1975; Tejwani et al., 1976; Pedrosa et al., 1977; Benkovic et al., 1978a,b; Pontremoli et al., 1979).

The binding stoichiometry for Mg^{2+} ion is uncertain. The presence of two distinct sets of binding sites for Mg^{2+} was reported at pH 7.2 and 9.1 in the absence of EDTA, but only one set of binding sites in the presence of EDTA at both pH 7.2 and 9.1 was reported (Tashima & Yoshimura, 1975). It is unclear whether the two sets of binding sites refer to two sites per monomer or to two sets of binding sites among the four sites of the tetramer molecule. A more recent study reported that only one Mg^{2+} was bound at each active site at pH 9.5 (Liu & Fromm, 1990).

Our work confirms that in the presence of the α analogue AhG-1,6-P_2 there are two metal binding sites for Zn^{2+} or Mn^{2+} at the active site, assigned as site 1 and site 2. At present we avoid using the terms "structural metal" and "catalytic metal" to describe the metal binding sites until their role in the mechanism is further clarified. However, only one Mg^{2+} near the metal site 1 was found in either the α or the β analogue complexes. When the $MgSO_4$ concentration used for preparing the crystals was increased from 5.0 to 20.0 mM, Mg^{2+} still occupies only the metal site 1 in the α analogue complex. In the presence of the β analogue AhM-1,6-P_2 one Mn^{2+} was found and it was very near the metal site 1.

The enzyme activated with 5.0 mM or less $MgSO_4$ is inhibited by low concentration, up to 10 μM, of Zn^{2+}. The degree of inhibition is 50% at 0.3 μM and 83% at 1.0 μM (Tejwani et al., 1976). Similar inhibition, perhaps by the same mechanism, by zinc ion at low concentration was observed using 20 μM Mn^{2+} instead of 5.0 mM Mg^{2+} as activator (Tejwani et al., 1976). This zinc inhibition could be overcome by increasing the Mg^{2+} concentration to 100 mM. Since the relative specific activities of Fru-1,6-Pase activated by Mg^{2+}, Mn^{2+}, and Zn^{2+} are 6:2:1 in the presence of EDTA (Benkovic & deMaine, 1982, and references cited therein), it is reasonable to postulate that some of the zinc inhibition reflects the intrinsic changes in activity from the Mg^{2+}- or the Mn^{2+}-activated enzyme relative to the Zn^{2+}-activated enzyme. Such a displacement is reasonable in view of the high affinity for Zn^{2+}: K_d = 0.34 μM at the high affinity site (Tejwani et al., 1976); moreover, this K_d value is identical to the value of K_i for Zn^{2+} in above systems (Tejwani et al., 1976; Pedrosa et al., 1977). Other factors may be also involved, because the

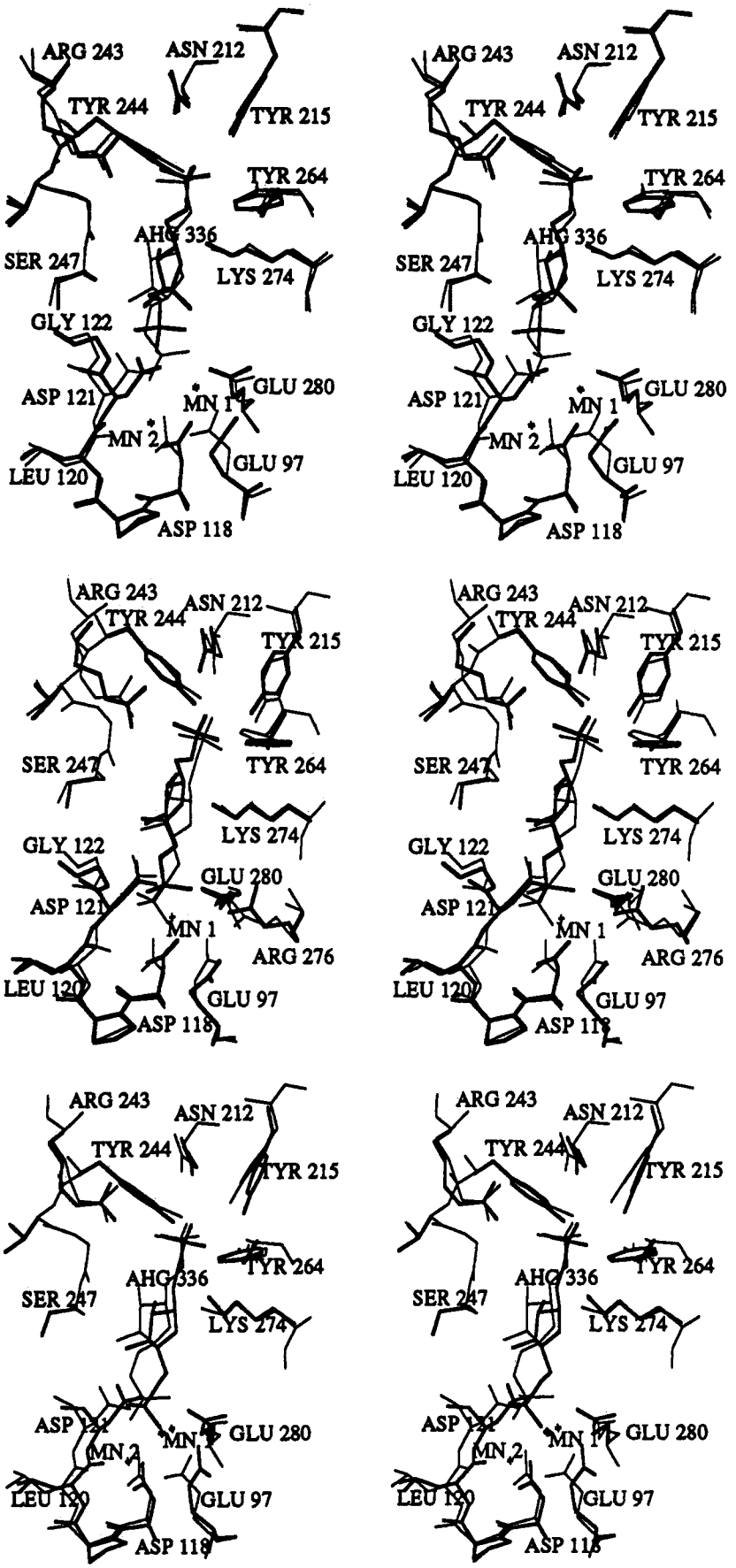

FIGURE 8: Superposition of active sites between substrate and analogue complexes and between analogue complexes: (a, top) AhG-1,6-P_2–Mn^{2+}–Fru-1,6-Pase, for which the Mn^{2+} ions are shown as crosses and the α anomer of substrate Fru-1,6-P_2 from the metal-free complex is drawn with thick lines; (b, middle) AhM-1,6-P_2–Mn^{2+}–Fru-1,6-Pase, for which Mn^{2+} is shown as a cross and the β anomer of substrate Fru-1,6-P_2 from the metal-free complex is drawn with thick lines; (c, bottom) superposition of the α and the β analogues, in which thick lines represent side chains from the β analogue complex and thin lines are residues from the α analogue complex; Mn^{2+} ions are shown as crosses in the lower middle of the picture. For clarity, Met-248, buried by the ligands, is omitted.

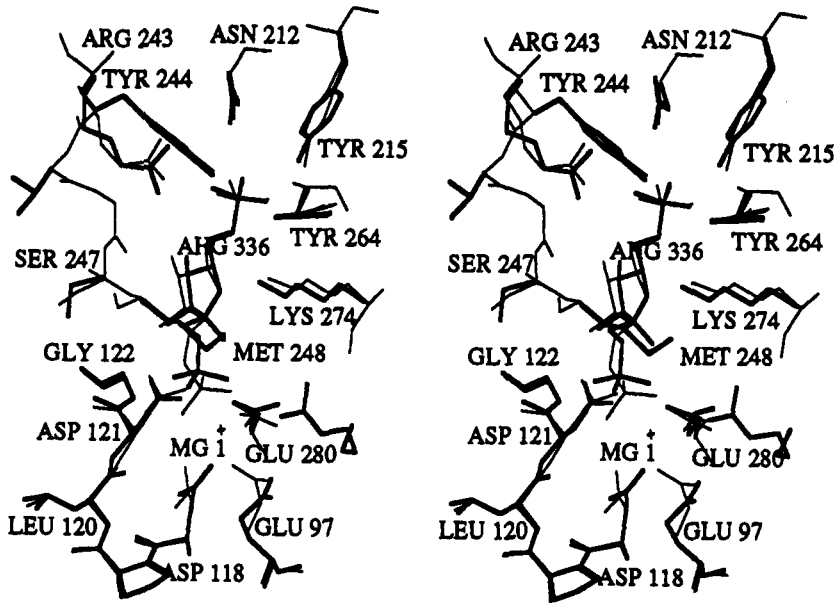

FIGURE 9: Superposition of the active sites. Thick lines represent the α monomer of Fru-1,6-P_2 and side chain atoms from substrate complex in the absence of metal ions. Thin lines denote residues from the α analogue complex AhG-1,6-P_2–Mg^{2+}–Fru-1,6-Pase; the Mg^{2+} ion is shown as a cross in the lower middle of the picture.

effects when two metals are present are not simply additive, as illustrated in systems containing Mg^{2+}/Zn^{2+} or Mn^{2+}/Zn^{2+} (Benkovic et al., 1978a).

The total concentration of Mg^{2+} in liver cells is reported to be 10.4 mM, and that of free Mg^{2+} is measured at 0.6–1.3 mM (Veloso et al., 1973). The total concentration for Mn^{2+} and Zn^{2+} in liver cells is 90 and 100 μM, respectively (Thiers & Vallee, 1957). If we assume that about 10% of these metals is free, the concentrations of all three metals are close to the K_m values for Mg^{2+} (0.64 mM; Nimmo & Tipton, 1975), Mn^{2+} (15 μM; Benkovic et al., 1978a), and Zn^{2+} (5 μM; Tejwani, 1976). It is therefore possible that the enzyme is regulated by the relative ratios of two or three of these metal ions; possibly all three metals are physiologically important.

Each of the three divalent metal ions shows some inhibition at high concentrations, although the characteristics differ. High Mg^{2+} concentration inhibits the enzyme activity only at low concentrations of Fru-1,6-P_2; at high concentrations of Fru-1,6-P_2 where substrate inhibition occurs, Mg^{2+} acts as an activator (Marcus et al., 1973). This effect is attributed to the formation of an unbound inactive metal substrate complex $(Mg–Fru\text{-}1,6\text{-}P_2)^-$, which lowers the effective concentration of substrate. For this system the value of 8 mM of $K_i(Mg^{2+})$ is the same as the K_d value of the $(Mg–Fru\text{-}1,6\text{-}P_2)^-$ complex reported by McGilvery (1965).

The inhibition of the enzyme at high concentration of Mn^{2+} was attributed to binding of the binary complex $(Mn–Fru\text{-}1,6\text{-}P_2)^-$ at an allosteric site (Libby et al., 1975). Although at higher concentrations the substrate, substrate analogues (this work), and product (Ke et al., 1991a) do bind at the AMP site with low occupancy, no metals were found in the AMP site. The physiological effect of the binding of substrate at the AMP site is not clear, and this binding does not cause the R to T transition. Our crystal structures show no significant structural changes at the AMP site when substrate or analogues bind at this regulatory site.

(*c*) *Catalytic Mechanisms.* The results from binding and kinetic studies suggested a kinetic model in which each enzyme subunit independently binds to the first metal ion at the high affinity site, then to the substrate Fru-1,6-P_2 and the second metal ion at the low affinity site, followed by subsequent hydrolysis of Fru-1,6-P_2 (Libby et al., 1975; Caparelli et al., 1978; Dudman et al., 1978; Benkovic et al., 1978b). Comparisons of active sites between the α Fru-1,6-P_2–Fru-1,6-Pase and AhG–Mg–Fru-1,6-Pase (Figure 9), as well as between AhG–Mg–Fru-1,6-Pase and AhG–Mn–Fru-1,6-Pase (Figure 10), indicate that binding of the first metal at site 1 requires little conformational change other than the repositioning of the 1-phosphate group of substrate or its analogue (Figure 9). However, binding of the second metal at the site 2 requires reorientation of the side chain of Glu-97, additional movement of main chain atoms of Leu-120 and Asp-121 and of their side chain atoms by 0.5–0.8 Å (Figure 10), and the presence of the 1-phosphate group of the substrate or its analogues. These observations, though not definite proof, are consistent with the above binding sequence.

We propose the following catalytic mechanism on the basis of the results from this work and those from binding and kinetic studies reported in the literature. The active site of the substrate metal complex is modeled by replacing AhG-1,6-P_2 with α-Fru-1,6-P_2 in the ternary complex AhG-1,6-P_2–M–Fru-1,6-Pase (M = Mn^{2+} or Zn^{2+}). This mechanism applies to systems using Mn^{2+} or Zn^{2+} as activator where the existence of two metal ions is supported by stoichiometric binding studies (Libby et al., 1975; Tejwani et al., 1976; Pedrosa et al., 1977; Benkovic et al., 1978a) and by X-ray structural analysis (this work). A schematic representation of this mechanism is given in Figure 11.

On the basis of the findings that two Mn^{2+} or Zn^{2+} ions are bound in the presence of the α analogue while only one metal ion is bound in the presence of the β analogue, the true substrate form is most likely the α anomer. Two metal ions of Mn^{2+} or Zn^{2+} at both metal sites 1 and 2 are required to carry out the hydrolysis of the substrate.

Initially, the C2-hydroxyl group donates an intramolecular hydrogen bond to the ester oxygen O1 (the distance between the two oxygen atoms is 2.5 Å). The ester oxygen O1 also interacts with the main chain NH of Gly-122. The carbonyl oxygen of Leu-120 is bound to the metal 2 as seen in crystal structures of ternary complexes, AhG-1,6-P_2–M–Fru-1,6-Pase (M = Mn^{2+} or Zn^{2+}).

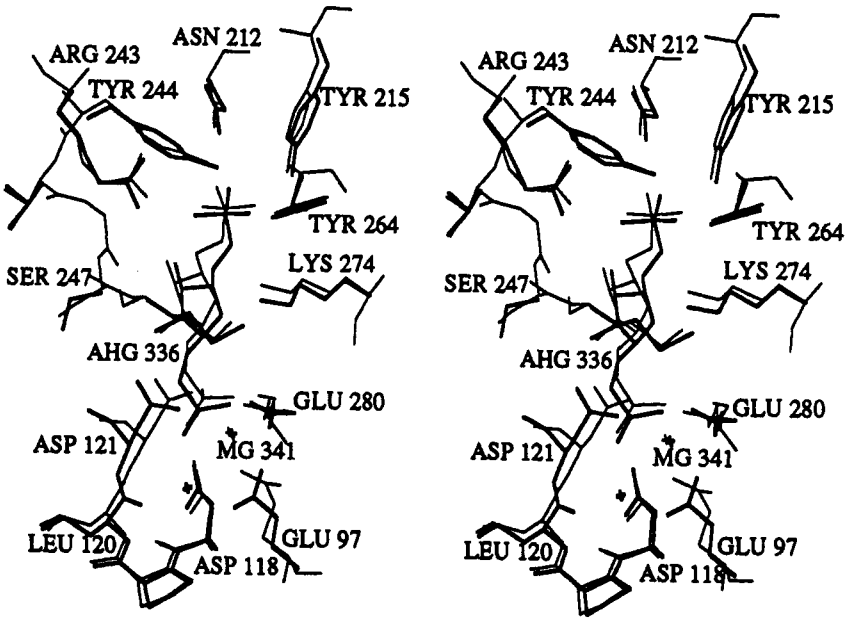

FIGURE 10: Superposition of the active sites of the α analogue AhG-1,6-P_2 complexed with Mg^{2+} and Mn^{2+}. Thick lines represent side chain atoms from the Mn^{2+} complex. Thin lines denote residues from the Mg^{2+} complex. The Mn^{2+} ions are shown as two thick crosses and the Mg^{2+} ion is shown as a thin cross in the lower middle of the picture. Note that the Mg^{2+} is very near the Mn^{2+} at site 1. For clarity, Met-248, buried by the substrate, is omitted.

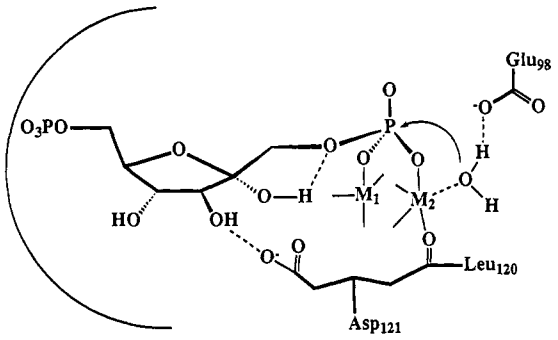

FIGURE 11: Schematic representation of features of one proposed catalytic mechanism when two metal ions, M1 and M2, are involved. Bridging ligands Glu-97 and Asp-118 and the terminal ligand Glu-280 on metal 1 are implied by the terminal lines emanating from the metal ions. Proposed nucleophilic attack by oxygen of H_2O or incipient OH^- on the phosphorus of the 1-phosphate may be assisted by proton transfer from this H_2O to Glu-98. Proton transfer to the bridging oxygen O1 may be assisted by Asp-121 and the C2-hydroxyl group.

From model building, we postulate that a water molecule is activated by binding to the metal ion 2 in a position for in-line nucleophilic attack at the 1-phosphate from the direction opposite to that of the scissile P–O bond. This attack could be facilitated by the side chain of Glu-98 which is 4.5 Å from the metal ion 2 and could deprotonate the water molecule. The metal ion 2 could become 5-coordinated, or the carbonyl oxygen of Leu-120 could be displaced to preserve the tetrahedral geometry.

The 1-phosphate group including the ester oxygen O1 makes several important polar interactions: (1) the direct coordination to the two metal ions; (2) the intramolecular hydrogen bonding between the C2-hydroxyl group and the ester oxygen O1; and (3) the hydrogen bond interaction between the ester oxygen O1 and the main chain NH group of Gly-122. All three interactions act to orient various groups into proper positions for activation and catalysis.

The side chain of Asp-121 is completely buried in the presence of the substrate or its analogue. Consequently, its pK_a might thereby be raised several units to a value close to neutral pH. Since the main chain segment of Leu-120 and Asp-121 is relatively flexible (Figure 8), Asp-121 could reorient slightly during catalysis so that the un-ionized carboxyl group could form a hydrogen bond to the C2-hydroxyl group of the substrate (distances between the carboxyl oxygen of Asp-121 to the C2-hydroxyl oxygen are from 3.2 to 3.4 Å in four independent sites). Alternatively, Asp-121 could form a new hydrogen bond between its un-ionized carboxyl group and the ester oxygen of the substrate (distances from the side chain carboxyl oxygen of Asp-121 to the ester oxygen O1 are 2.7 to 3.2 Å in four independent sites of two complexes). In either case, this new hydrogen bond interaction would cause the protonation of the ester oxygen O1, thus weakening the P–O bond.

One role of the metal ions in this mechanism may be to position the 1-phosphate group into the correct conformation so that the ester oxygen O1 could receive hydrogen bonds from the C2-hydroxyl group of the substrate, from the main chain NH group of Gly-122, and possibly also from the side chain carboxyl group of Asp-121. In addition, the metal ion 2 would help to activate the water molecule for nucleophilic attack at the phosphorus center.

During the catalysis, if the rate-limiting step is the nucleophilic attack, then the pH dependency of the enzyme activity will be correlated to the pK_a of the nucleophile. The observed optimum pH for Fru-1,6-Pase from various sources is metal dependent: from 7.0 to 7.4 for Mg^{2+} (Van Tol et al., 1972; Colombo & Marcus, 1973; Tashima & Yoshimura, 1975) and 8.2 for Mn^{2+} (deMaine & Benkovic, 1972; Tashima & Yoshimura, 1975). There is no direct measurement of the pH dependency of Zn^{2+}-activated enzyme, but indirect evidences suggest that the optimum pH would be near 9 or above (Tashima & Yoshimura, 1975). When EDTA is added to the buffer used for activity assay, the enzyme activated by Mg^{2+} usually shows an increase of activity and a shift of optimum pH from 8.5 or above to 7.4. This effect of EDTA on the activity was attributed to the removal of an inhibitory metal ion, most probably Zn^{2+}, from the samples (deMaine & Benkovic, 1972; Tejwani et al., 1976). These observations are in agreement with the assumption that a metal bound

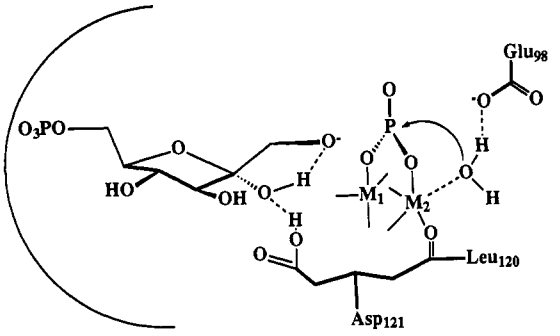

FIGURE 12: Pyrophosphate mechanism. In the AGMN and AGZN substrate analogues the distances from M_1 to the scissile oxygen of the ribose is 4.5 ± 0.5 Å and to the nearest oxygen of Asp-121 is 2.7 Å. Small conformational changes could occur so that one or the other could become a metal ligand.

water is involved in the nucleophilic attack of the phosphate and this step is the rate-limiting step.

In comparison to the catalytic mechanism of the alkaline phosphatase based on the structure of Kim and Wyckoff (1991; Coleman, 1992), we note that both zinc ions, 3.9 Å apart, in alkaline phosphatase are involved in a two-step catalysis with a phosphoseryl-enzyme intermediate. In the first step, Zn(1) activates the leaving group by coordination to the ester oxygen, while Zn(2) coordinates to one phosphate oxygen and the other two phosphate oxygens form hydrogen bonds with the guanidinium group of Arg-166. Ser-102 is the nucleophile and occupies the position opposite to that of the leaving group. In the second step, a water molecule or a hydroxide molecule on Zn(1) attacks, while the Zn(2) coordinates to the ester oxygen of the phosphoseryl intermediate. Arg-166 remains hydrogen bonded to the same two phosphate oxygens as in the first step.

Thus, the major differences between mechanisms of Fru-1,6-Pase and alkaline phosphatase are as follows. Fru-1,6-Pase uses only one of the two metal ions in a one-step mechanism, while alkaline phosphatase uses both metal ions in a two-step mechanism involving a phosphoseryl intermediate. In both enzymes, the nucleophiles are metal bound water molecule or hydroxide ion. The two metal ions coordinate to two phosphate oxygens in Fru-1,6-Pase but to ester oxygens in alkaline phosphatase. The former coordination may be important in positioning the 1-phosphate group for an effective nucleophilic attack, while the latter for activating the ester oxygen. For Fru-1,6-Pase, activation of the ester oxygen is most likely achieved by hydrogen bonding of the ester oxygen with the NH of Gly-122, with the C2-hydroxy of the substrate, and with the side chain of Asp-121.[3] A covalent intermediate, phosphseryl-102, is formed during catalysis by alkaline phosphatase. However, there is no evidence for a covalently bound phosphoenzyme intermediate in catalysis by Fru-1,6-Pase.

We do not know in our essentially S_N2 mechanism if a stable intermediate with a five-coordinated phosphorus center is formed. An alternative S_N1 mechanism involves the cleavage of the ester P–O bond as the initial step, which might be promoted by preprotonation of the ester oxygen by the C2-hydroxyl of the substrate, the NH of Gly-122, or the side chain carboxyl of Asp-121. This reaction yields Fru-6-P and the incipient or actual intermediate metaphosphate anion [PO_3^-] (Butcher & Westheimer, 1955; Kirby & Jencks, 1965; Kirby & Varvoglis, 1967; Miller & Westheimer, 1966). For the inversion of configuration at the phosphorus center to occur (Domanico et al., 1985), this metaphosphate intermediate would have to remain bonded to the enzyme, i.e., to two metal ions, as it is rapidly transformed in a stereospecific manner to form $H_2PO_4^-$ by a H_2O molecule. This water molecule could be activated by binding to the metal 2 and by proton transfer to a nearby general base Glu-98. However, we could not find a water near the metal site 2 in our X-ray structures. This could be due to the relatively low resolution of this study or to weak binding of a water molecule to a loosely bound metal ion. It is also possible that metal coordination of a water molecule requires rearrangement of electron distribution[4] occurring only during the catalysis.

In organic model systems, most phosphate mono- and diesters hydrolyze through a dissociative S_N1 mechanism (Westheimer 1968; Benkovic & Schray, 1973; Knowles, 1980). In the enzyme-catalyzed reactions, the S_N2 mechanism can become more favorable due to the proximity of the participating reacting groups at the enzyme active site. This condition is not readily available in model systems.

In the α analogue AhG-1,6-P_2 complexes with Mn^{2+} or Zn^{2+}, the side chain carboxyl group of Asp-121 is not bound to the metal ion at site 1 and thus is free to participate in the hydrogen bond interactions with the substrate analogue. However, in the β analogue AhM-1,6-P_2 complexes, the side chain carboxyl group of Asp-121 is coordinated to either Mg^{2+} or Mn^{2+} ion at the site 1, rendering it unavailable for further hydrogen bonding to the C2-hydroxyl or the ester oxygen atoms. These observed differences are consistent with the proposed mechanism. However, in the α analogue AhG-1,6-P_2 complex with Mg^{2+}, the side chain carboxyl group of Asp-121 is also coordinated to the Mg^{2+} ion, again indicating indirectly that there may be a modified catalytic mechanism for the Mg^{2+} complex.

This work establishes that there is only one Mg^{2+} ion at the active site in the presence of either the α or β substrate analogue at pH 7.4 at 5.0 mM Mg^{2+} and even at 20.0 mM Mg^{2+} concentration for the α analogue. However, we do not know whether the enzyme in the crystal is enzymatically active when only one Mg^{2+} is bound at the active site. Whether a second Mg^{2+} at metal site 2 is required to activate the enzyme is still open to debate. It is also conceivable that Mg^{2+} might activate the enzyme via an entirely different mechanism in which only one Mg^{2+} ion is necessary or that the Mg^{2+} system might proceed without inversion at the 1-phosphate or even might have different anomeric specificity. The Mg^{2+} is five coordinated in both the α and the β analogue complexes, whereas the Mn^{2+} or Zn^{2+} is four coordinated in the α analogue complexes. The smaller ionic radius of the Mg^{2+} ion compared to the ionic radii of Mn^{2+} or Zn^{2+} may mean that it is more difficult for Mg^{2+} to take on an additional H_2O molecule as ligand than for Mn^{2+} or Zn^{2+}. More experiments are needed to answer these specific questions regarding the role of the Mg^{2+} in the mechanism.

When Lys-274 is mutated to Ala-274, the mutant protein has the same specific activity as does the wild-type protein, while the K_m for the substrate is decreased 20 times (Raafat et al., 1992). Thus, Lys-274 plays a role in binding of the substrate but is not involved in the catalytic steps but rather

[3] Also, in bovine pancrease ribonuclease, activation of leaving phosphate is achieved by hydrogen bonding of ester oxygens to side chains of histidines.

[4] For example, development of a metaphosphate anion in the modified S_N1 reaction may reduce the binding interaction between the metaphosphate oxygens and the metal ion, leaving the metal ion more acidic to bind and activate a water molecule.

contacts the C2 phosphate group of Fru-2,6-P_2 and is essential for binding this regulatory ligand.

Our proposed catalytic mechanisms of the neutral form of Fru-1,6-Pase are consistent with many findings from the literature. It agrees with the experimental data that the true substrate is the α anomer and gives a plausible explanation for the absolute requirement of the C2-hydroxyl group of substrate. It is consistent with the results of metal binding studies that there are two metal binding sites per monomer for Mn^{2+} or Zn^{2+}. It is also consistent with the result that the zinc concentration up to 10 μM inhibits the Mg^{2+}- or Mn^{2+}-activated enzyme. This mechanism also implies that the hydrolysis takes place with inversion at the phosphorus atom, the same conclusion that was obtained from isotope labeling studies (Domanico et al., 1985).

More studies, especially those based on the site-directed mutagenesis technique, are necessary to modify or validate this mechanism. Also, further crystallographic studies at various pH values and concentrations of metal ions and at higher resolution are necessary to better define the roles of those residues in the active site. Some candidates for mutation include Glu-97, Glu-98, Asp-118, and Asp-121.[5] Kinetic studies using novel substrate analogues will continue to provide valuable information about the mechanism. Analogues having fixed anomeric conformation and a proton donor, such as a hydroxyl or a sulfhydryl group on the C2 atom, will reveal more information about the role of the C2-hydroxyl group in catalysis and further delineate the anomeric requirement of the active site. Further studies on the T state complexes of substrate or substrate analogue, AMP, and metal ions will elucidate how the allosteric inhibitor AMP and metal ions interact with each other to regulate the enzyme activity and how the signal propagates from the allosteric site to the active site.

ACKNOWLEDGMENT

We thank Drs. S. Sobottka and R. Kretsinger for the use of the multiwire X-ray area detector at the Biotechnology Resource, University of Virginia. We also thank Drs. Ray Stevens and Mark D. Erion and Professors Simon J. Pilkis and Herbert J. Fromm for helpful discussions.

REFERENCES

Benkovic, S. J., & Schray, K. J. (1973) *Enzymes, 3rd Ed. 8*, 201–238.

Benkovic, S. J., & deMaine, M. M. (1982) *Adv. Enzymol. Relat. Areas Mol. Biol. 53*, 45–82.

Benkovic, P. A., Bullard, W. P., deMaine, M. M., Fishbein, R., Schray, K. J., Steffens, J. J., & Benkovic, S. J. (1974) *J. Biol. Chem. 249*, 930–931.

Benkovic, P. A., Caperelli, C. A., deMaine, M. M., & Benkovic, S. J. (1978a) *Proc. Natl. Acad. Sci. U.S.A. 75*, 2185–2189.

Benkovic, P. A., Frey, W. A., & Benkovic, S. J. (1978b) *Arch. Biochem. Biophys. 191*, 719–726.

Blum, M., Metcalf, P., Harrison, S. C., & Wiley, D. C. (1987) *J. Appl. Crystallogr. 20*, 235–242.

Brünger, A. T., Kuriyan, J., & Karplus, M. (1987) *Science 235*, 458–460.

Butcher, W. W., & Westheimer, F. H., (1955) *J. Am. Chem. Soc. 77*, 2420–2424.

Caperelli, C. A., Frey, W. A., & Benkovic, S. J. (1978) *Biochemistry 17*, 1699–1704.

[5] Recently, Professor S. Pilkis' group has made the mutations of Asp-118 to Ala-118 and Asp-121 to Ala-121 in human liver Fru-1,6-Pase, and in both cases the mutated protein is found to have greatly diminished catalytic activity (Raafat El-Maghrabi et al., manuscript in press).

CCP4 (1979) The SERC (U.K.) Collaborative Computing Project No. 4, A Suite of Programs for Protein Crystallography, distributed from Daresbury laboratory, Warrington, WA 4AD, U.K.

Cerrini, S., Coiro, V. M., Lamba, D., & Bisso, G. M. B. (1986) *Carbohydrate Res. 147*, 183–190.

Coleman, J. E. (1992) *Annu. Rev. Biophys. Biomol. Struct. 21*, 441–483.

Colombo, G., & Marcus, F. (1973) *J. Biol. Chem. 248*, 2743–2745.

deMain, M. M., & Benkovic, S. J. (1972) *Arch. Biochem. Biophys. 152*, 272–279.

Domanico, P. L., Rahil, J. F., & Benkovic, S. L. (1985) *Biochemistry 24*, 1623–1628.

Dudman, N. P. B., deMaine, M. M., & Benkovic, S. J. (1978) *J. Biol. Chem. 253*, 5712–5718.

Findlay, D., Herries, D. G., Mathias, A. P., Rabin, B. R., & Ross, C. A. (1961) *Nature (London) 190*, 781.

Fox, G. C., & Holmes, K. C. (1966) *Acta Crystallogr. 20*, 886–891.

Frey, W. A., Fishbein, R., deMaine, M. M., & Benkovic, S. J. (1977) *Biochemistry 16*, 2479–2884.

Grazi, E., Accorsi, A., & Pontremoli, S. (1971) *J. Biol. Chem. 246*, 6651–6654.

Han, P. F., Owen, G. S., & Johnson, J., Jr. (1975) *Arch. Biochem. Biophys. 168*, 171–179.

Hartman, F. C., & Barker, R. (1965) *Biochemistry 4*, 1068.

Ikeda, T., Kimura, K., Hama, T., & Tamaki, N. (1980) *J. Biochem. 87*, 179–185.

Jones, T. A. (1982) in *Computational Crystallography* (Sayer, D., Ed.) pp 303–317, Oxford, London.

Ke, H., Thorpe, C. M., Seaton, B. A., Lipscomb, W. N., & Marcus, F. (1990a) *J. Mol. Biol. 212*, 513–539; *214*, 950 (correction).

Ke, H., Zhang, Y., & Lipscomb, W. N. (1990b) *Proc. Natl. Acad. Sci. U.S.A. 87*, 5243–5247.

Ke, H., Liang, J., Zhang, Y., & Lipscomb, W. N. (1991a) *Biochemistry 30*, 4412–4420.

Ke, H., Zhang, Y., Liang, J., & Lipscomb, W. N. (1991b) *Proc. Natl. Acad. Sci. U.S.A. 88*, 2989–2993.

Kim, E. E., & Wyckoff, H. W. (1991) *J. Mol. Biol. 218*, 449–464.

Kirby, A. J., & Jencks, W. P., (1965) *J. Am. Chem. Soc. 87*, 3209–3216.

Kirby, A. J., & Varvoglis, (1967) *J. Am. Chem. Soc. 89*, 415–423.

Kirtley, M. E., & Dix, J. (1971) *Arch. Biochem. Biophys. 147*, 647–652.

Knowles, J. R. (1980) *Annu. Rev. Biochem. 49*, 877–919.

Liang, J.-Y., Huang, S., Zhang, Y., & Lipscomb, W. N. (1992) *Proc. Natl. Acad. Sci. U.S.A. 89*, 2404–2408.

Libby, C. B., Frey, W. A., Villafranca, J. J., & Benkovic, S. J. (1975) *J. Biol. Chem. 250*, 7564–7573.

Lipscomb, W. N. (1991) *Chemtracts 2*, 1–15.

Liu, F., & Fromm, H. J. (1990) *J. Biol. Chem. 265*, 7401–7406.

Marcus, C. J. (1976) *J. Biol. Chem. 251*, 2963–2966.

Marcus, C. J., Geller, A. M., & Byrne, W. L. (1973) *J. Biol. Chem. 248*, 8567–8573.

McGilvery, R. W. (1965) *Biochemistry 4*, 1924–1930.

Midelfort, C. F., Gupta, R. K., & Rose, I. A. (1976) *Biochemistry 15*, 2178–2185.

Miller, D. L., & Westheimer, F. H. (1966) *J. Am. Chem. Soc. 88*, 1507–1511.

Narendra, N., Seshadri, T. P., & Viswamitra, M. A. (1985) *Acta Crystallogr. C41*, 31–34.

Nimmo, H. G., & Tipton, K. F. (1975) *Eur. J. Biochem. 58*, 567–585.

Pedrosa, F. O., Pontremoli, S., & Horecker, B. L. (1977) *Proc. Natl. Acad. Sci. U.S.A. 74*, 2742–2745.

Pontremoli, S., Grazi, E., & Accorsi, A. (1969) *Biochem. Biophys. Res. Commun. 37*, 597–602.

Pontremoli, S., Melloni, E., Salamino, F., Sparatore, B., & Horecker, B. L. (1978) *Arch. Biochem. Biophys. 188*, 90–97.

Pontremoli, S., Sparatore, B., Salamino, F., Melloni, E., & Horecker, B. L. (1979) *Arch. Biochem. Biophys. 194*, 481–485.

Raafat El-Maghrabi, M., Austin, L. R., Correia, J. J., & Pilkis, S. J. (1992) *J. Biol. Chem. 267*, 6526–6530.

Racker, E., & Shroeder, E. A. R. (1958) *Arch. Biochem. Biophys. 74*, 326–344.

Sobottka, S. E., Cornic, G. G., Kretsinger, R. H., Rains, R. G., Stephens, W. A., & Weissman, L. J. (1984) *Nucl. Instrum. Methods 220*, 575–581.

Tashima, Y., & Yoshimura, N. (1975) *J. Biochem. 78*, 1161–1169.

Tejwani, G. A. (1983) *Adv. Enzymol. Relat. Areas Mol. Biol. 54*, 121–194.

Tejwani, G. A., Pedrosa, F. O., Pontremoli, S., & Horecher, B. L. (1976) *Proc. Natl. Acad. Sci. U.S.A. 73*, 2692–2695.

Thiers, R. E., & Vallee, B. L. (1957) *J. Biol. Chem. 226*, 911–920.

Underwood, A. H., & Newsholme, E. A. (1965) *Biochem. J. 95*, 767–774.

Van Tol, A., Black, W. J., & Horecker, B. L. (1972) *Arch. Biochem. Biophys. 151*, 591–596.

Veloso, D., Guynn, R. W., Oskarsson, M., & Veech, R. L. (1973) *J. Biol. Chem. 248*, 4811–4819.

Westheimer, F. H. (1968) *Acc. Chem. Res. 1*, 70–78.